Fast, high resolution T2* mapping using 3D MGE and 3D EPI, with 3D correction for macroscopic dephasing effects

S. Robinson[1], M. Barth[2], and J. Jovicich[1]

[1]Centre for Mind/Brain Sciences, University of Trento, Trento, Trentino, Italy, [2]Centre for Cognitive Neuroimaging, Donders Institute for Brain, Cognition and Behaviour, Nijmegen, Netherlands

Introduction: T_2* relaxation reflects both non-reversible microscopic T_2 processes and reversible T_2' processes. Whilst T_2' is influenced by intravoxel dephasing due to such clinically interesting, tissue-specific quantities as local iron concentration, its reliability in comparative and longitudinal studies is limited by the dephasing effect of static magnetic field gradients, which are dominant in some brain regions [1]. Signal decay in the prescence of macroscopic field variations may be modelled as

$$S(TE) = S_0 \exp(-TE/T^*_{2\_mes}).F(TE), \text{ where } F(TE) = \text{sinc}\left(\Delta\varpi_x TE/2\right)\text{sinc}\left(\Delta\varpi_y TE/2\right)\text{sinc}\left(\Delta\varpi_z TE/2\right)$$

where $T^*_{2\_mes}$ includes both T_2 contributions and T_2' contributions on the scale of the voxel size (mesocopic), but not macroscopic B_0 effects, and $\Delta\omega_i$ is the field gradient along the imaging axis i, which may be calculated from inherent phase information [2]. It has recently been demonstrated that this formulation may be used to correct dephasing due to gradients in the slice direction using a 2D multi gradient echo (MGE) acquisition [3]. We have developed this into a fast, high resolution technique suitable for reproducible T_2* relaxometry of small structures by implementing the method with a number of high resolution methods which we compare here: isotropic 2D MGE, 3D segmented EPI and 3D MGE acquisitions (the latter with and without acceleration) and by correcting for field gradient effects along all three imaging axes. Results are assessed in the basal ganglia, structures which show a range of T_2* values due differing iron concentrations [4] and which are of clinical interest in a range of pathologies such as Parkinson's disease, Alzheimer's disease and multiple sclerosis.

Materials and Methods: Data were acquired with a Bruker Medspec 4T scanner with an 8-channel head coil. Whole-brain multi-echo data, with 10 echoes in the range 5 to 41 ms in 4 ms intervals, were acquired with 5 sequences i) 2D-MGE with 1x1x5 mm voxels, similar to that used in [3], TA = 2'10", and 4 sequences with isotropic 1x1x1 mm^3 voxels: ii) 2D-MGE, TA = 11'5" iii) 3D EPI, EPI_factor = 7, TA = 14'48". iv) 3D MGE, TA = 8'41" v) 3D MGE, GRAPPA factor = 2, TA = 5'21". Fat saturation was used and data was recorded separately for all 8 channels.

Analysis: Phase data from individual receiver channels from the first two echoes of each dataset were spatially unwrapped and used to create single-channel field maps. These were combined, weighting each fieldmap by the square of the corresponding magnitude image [5]. Consistency over channels (standard deviation) was used to exclude unreliable voxels, which were replaced by the median value in a 3x3 kernel [6]. The resulting field maps were used to calculate field gradients along imaging axes and the value of the function F(TE) at each echo time. Decay data were divided by F(TE) to correct for decay originating from macroscopic B_0 variations. Both uncorrected and corrected data were fit with a single exponential decay. In the corrected data, echoes were included in the fit for which F(TE) > 0.1. T_2^* values were assessed in an occipital grey matter ROI (OC), and 3D ROIs in the red nuclei (RN), the substantia nigra (SN), the globus pallidus (G) and the putamen (P).

Results: In the 2D 5 mm slice thickness sequence (i), uncorrected T_2^* values were generally very short and the basal ganglia could not be well distinguished (Fig 1, top left). Both 2D sequences showed low values in dropout regions (blue arrows). The RN were circumscribed and well separated from the SN in all high resolution sequences (see labels on extract, Fig 1, far right). T_2^* values were consistent between sequences, as were the standard deviation of values in ROIs, indicating similar noise levels (Table 1). The 3D EPI sequence was most prone to rapid susceptibility changes, e.g. in the proximity of the middle and anterior cerebral arteries, where fits did not converge (white areas at green arrows). The correction for macroscopic dephasing led to increases in T_2^* of 22% in SN, 17% in RN – due to the proximity of the circle of Willis - but only 6% in P, 2% in G and 4 % in OC. The F(TE) gave effective removal of dephasing effects in some areas (Fig 2, at position of yellow arrows), returning T_2^* to values close to those in cortical grey matter in homogeneous regions, circa 40 ms (e.g. 22 ms corrected to 38 ms, Fig 2., right) but also increase noise substantially.

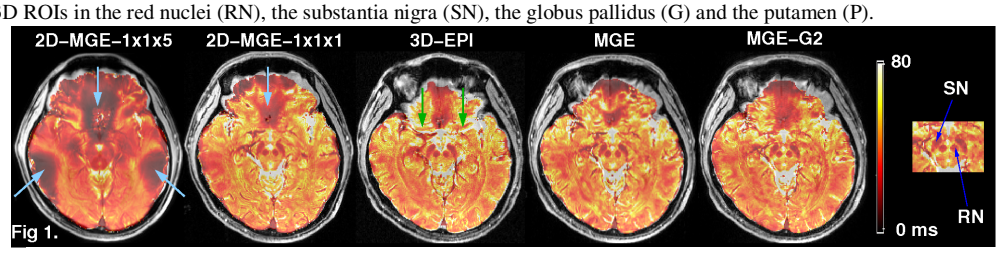

Fig 1.

	2D-EPI		3D-EPI		MGE		MGE-G2	
	T2*	T2*-F_cor	T2*	T2*-F_cor	T2*	T2*-F_cor	T2*	T2*-F_cor
Occipital Cortex	41.3 ± 5.4	42.7 ± 6.9	39.7 ± 6.0	40.9 ± 6.3	38.1 ± 4.1	39.5 ± 4.3	39.3 ± 5.3	41.3 ± 6.1
Putamen	30.6 ± 3.0	31.8 ± 3.1	34.2 ± 3.3	36.6 ± 4.0	32.5 ± 2.6	34.7 ± 4.3	32.9 ± 3.1	35.4 ± 3.9
Pallidum	20.3 ± 2.0	21.3 ± 2.1	22.0 ± 2.3	23.7 ± 2.0	17.8 ± 1.9	19.2 ± 2.4	20.7 ± 2.2	18.1 ± 9.8
Red Nuclei	24.7 ± 4.0	25.6 ± 3.0	25.3 ± 3.0	29.9 ± 5.4	25.3 ± 4.1	29.9 ± 6.7	25.7 ± 3.6	32.4 ± 8.7
Substantia Nigra	24.5 ± 3.3	26.1 ± 3.7	20.5 ± 2.5	23.6 ± 2.5	20.5 ± 3.1	23.1 ± 3.8	21.0 ± 3.1	31.9 ± 10.6

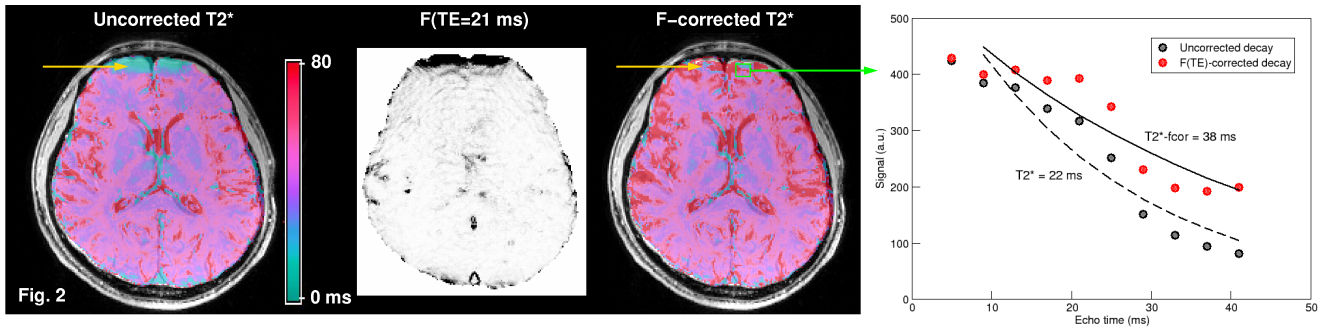

Fig. 2

Discussion and conclusion: The accelerated MGE sequence (MGE-G2) - the fastest sequence variant test - allowed reliable high resolution T_2^* mapping of the brain, and suffered no loss of accuracy with respect to the unaccellerated MGE sequence, and less vulnerability to field gradients than 2D MGE and 3D EPI. In the current implementation, isotropic submillimetre T_2* maps of the whole brain can be acquired in just over 5 minutes. Restricted slab imaging of the basal ganglia (e.g. with a 4 cm slice FOV) could be performed in approximately 2 minutes, making it a realistic means to study clinical groups with low tolerance. Calculation of F(TE) allows the correction of T_2* values in regions with moderate field gradients and the identification of unreliable voxels. Future work will include the use of higher acceleration factors and assessment of intersession consistency and the accuracy of the field gradient correction, particularly in regions of high field gradients.

Acknowledgment. Support for this research was provided in part by the government of the Provincia Autonoma di Trento, Italy, the private foundation Fondazione Cassa di Risparmio di Trento e Rovereto, and the University of Trento, Italy.

References: [1] Ordidge, R.J., et al., Magn Reson Med, 1994. **32**(3): p. 335. [2] Yablonskiy, D.A., Magn Reson Med, 1998. **39**(3): p. 417. [3] Dahnke, H., et al., Magn Reson Med, 2005. **53**(5): p. 1202. [4] Gelman, N., et al., Radiology, 1999. **210**(3): p. 759. [5] Bernstein, M.A., et al., Magn Reson Med, 1994. **32**(3): p. 330. [6] Robinson, S., Jovicich, J., Proc. 16th ISMRM, Toronto, 2008.